J|A|C|S
COMMUNICATIONS

Published on Web 02/27/2008

Conjugated Oligoelectrolyte Electron Transport/Injection Layers for Organic Optoelectronic Devices

Renqiang Yang,[†] Yunhua Xu,[†,‡] Xuan-Dung Dang,[†] Thuc-Quyen Nguyen,[†] Yong Cao,[‡] and Guillermo C. Bazan*,[†]

Department of Chemistry and Biochemistry, Department of Materials, Institute for Polymers and Organic Solids, University of California, Santa Barbara, California 93106, and Institute of Polymer Optoelectronic Materials and Devices, South China University of Technology, Guangzhou 510640, China

Received December 13, 2007; E-mail: bazan@chem.ucsb.edu

Conjugated polymers with pendant ionic groups (conjugated polyelectrolytes, CPEs)[1] or polar functionalities have gathered recent interest because they can function as very effective electron injection/transport layers (ETLs) in polymer light emitting diodes (PLEDs).[2,3] The mechanism of action remains under debate. One possibility involves lowering the injection barriers by the introduction of permanent dipoles between the cathode and the semiconducting layer. The net result is a shift of the vacuum levels at the interface with a corresponding modification of the work function or surface potential of the electrode.[4] Alternatively, in the case of CPEs, the applied bias under operating conditions provides the driving force for ion migration, which causes a redistribution of the internal field within the ETL.[5] Within this model, the device incorporates some of the characteristics of light-emitting electrochemical cells (LECs).[6] Despite these mechanistic uncertainties, the use of CPEs opens the possibility of using high work function and stable metals, such as Al, Ag, or Au, and the deposition of electrodes by printing techniques.[7] These considerations are relevant for the design of more efficient organic optoelectronic devices, including white-light emitting PLEDs that may be more power efficient than conventional lighting sources.

We show here that oligomers representative of CPE structures, i.e., conjugated oligoelectrolytes (COEs), show excellent function as ETLs. Relative to polymer-based materials, COEs provide better-defined molecular structures, in that they are not described by molecular weight distributions, and can be obtained in higher purity. Additionally, that there are no batch-to-batch variations in their structural properties should lead to more reproducible device fabrication protocols. We also show that, unlike previous observations for their polymeric counterparts,[5] the use of COEs leads to PLEDs with fast temporal responses in their current densities and light emission.

Shown in Scheme 1 are the synthesis and the structure of a hexacationic fluorene trimer with (*N*,*N*,*N*-trimethylammonium)hexyl substituents and tetrakis(1-imidazolyl)borate counterions (**FFF-BIm$_4$**). This structure is representative of three consecutive repeat units in the corresponding cationic poly(fluorene) species.[8] The choice of the **BIm$_4$** anion was made on the basis of the previous excellent ETL performance obtained with cationic CPEs containing this counterion.[9] The overall synthesis involves the Pd-mediated Suzuki cross coupling reaction of 2,7-bis(4,4,5,5-tetramethyl-1,3,2-dioxaborolan-2-yl)-9,9-bis(6′-bromohexyl)fluorene with 2-bromo-9,9-bis(6′-bromohexyl)fluorene[10] to form the conjugated core (step i in Scheme 1). The resulting fluorene trimer is soluble in common organic solvents, can be purified by standard chromatography, and was analyzed by NMR spectroscopy, mass spectrometry, and elemental analysis. Quaternization of the neutral trimer by using

Scheme 1. Synthesis and Molecular Structure of **FFF-BIm$_4$**[a]

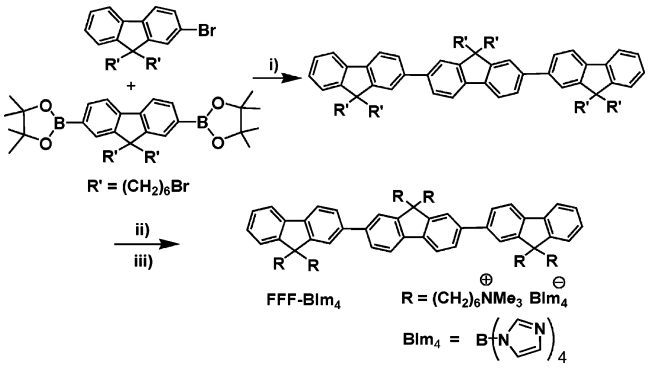

[a] Conditions: (i) $Pd(PPh_3)_4$, 2 M Na_2CO_3, toluene, reflux, 24 h; (ii) NMe_3, THF/methanol; (iii) dialysis with Na**BIm$_4$** in water.

trimethylamine in a THF/methanol solvent mixture (step ii), followed by exchange of bromide using Na**BIm$_4$** by dialysis in water (step iii), yields **FFF-BIm$_4$** in 75% overall yield. X-ray photoelectron spectroscopy (XPS) analysis confirmed quantitative replacement by **BIm$_4^-$**. **FFF-BIm$_4$** is soluble in polar solvents such as methanol, water, DMF, and DMSO.

To examine the use and performance of **FFF-BIm$_4$** as an ETL, we tested the performance of PLEDs with the architecture ITO/PEDOT:PSS/MEH-PPV/**FFF-BIm$_4$**/Al (PEDOT:PSS is poly(ethylenedioxy-thiophene):poly(styrenesulfonic acid); MEH-PPV is poly(2-methoxy-5-(2′-ethylhexyloxy)-1,4-phenylenevinylene)). Fabrication closely followed procedures developed for devices containing a CPE ETL.[9] The organic deposition steps were carried out by spin coating films from solution. No intermixing of the **FFF-BIm$_4$** (cast from methanol) and MEH-PPV (cast from toluene) layers was anticipated because of the orthogonal solubility of the two materials.[11−13] The cathode was deposited by thermal evaporation. Two control device structures were also fabricated, ITO/PEDOT:PSS/MEH-PPV/Ba/Al and ITO/PEDOT:PSS/MEH-PPV/Al. The former allows comparison against a device where ohmic contact (MEH-PPV/Ba) takes place between the cathode and MEH-PPV,[14] while the latter provides insight into how the **FFF-BIm$_4$** ETL modifies electron injection from the Al cathode.

Shown in Figure 1a are the current density−luminance−voltage (*J*−*L*−*V*) characteristics as a function of device structure. Insertion of the **FFF-BIm$_4$** ETL adjacent to Al gives rise to *J* and *L* that are higher than those observed when using Ba. The turn-on voltage is also lower. In these devices, the emission is evenly distributed (Supporting Information) and arises solely from the MEH-PPV layer. There is no emission in the case of ITO/PEDOT:PSS/MEH-PPV/Al, consistent with poorly balanced charge injection and thus ineffective electron injection. Examination of the luminous efficiency (cd/A) vs *J* characteristics shows that the **FFF-BIm$_4$**/Al

[†] University of California, Santa Barbara.
[‡] South China University of Technology.

10.1021/ja711068d CCC: $40.75

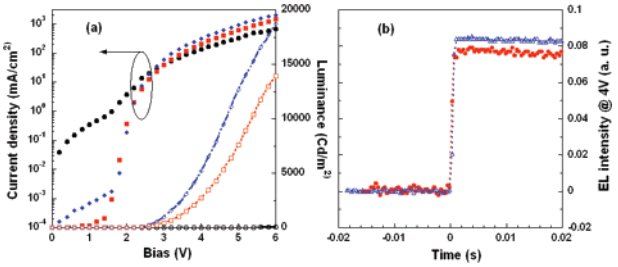

Figure 1. (a) $J-L-V$ characteristics of PLEDs with the following architectures: ITO/PEDOT:PSS/MEH-PPV/**FFF-BIm$_4$**/Al (blue diamonds), ITO/PEDOT:PSS/MEH-PPV/Ba/Al (red squares), and ITO/PEDOT:PSS/MEH-PPV/Al (black circles). (b) EL response at 4 V of ITO/PEDOT:PSS/MEH-PPV/**FFF-BIm$_4$**/Al (blue triangles) and the control device ITO/PEDOT:PSS/MEH-PPV/Ba/Al (red circles).

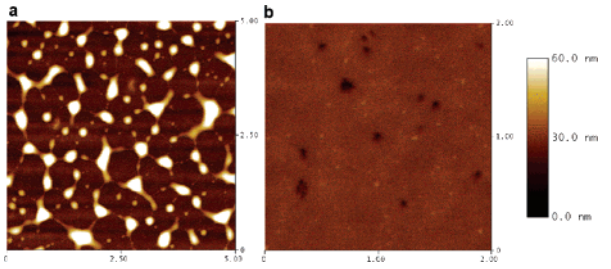

Figure 2. Topographic images obtained by AFM of the **FFF-BIm$_4$** layer cast atop MEH-PPV: (a) as cast and (b) in the region between two Al electrodes after metal deposition.

device is the most efficient (Supporting Information). For example, the cd/A observed at 200 mA/cm^2 as a function of the cathode are 1.66 (3.7 V) for **FFF-BIm$_4$**/Al, 1.32 (4.0 V) for Ba/Al, and 0.006 (4.4 V) for Al. The decay of the device performance over 1000 min was identical whether **FFF-BIm$_4$**/Al or Ba/Al was used as the cathode (Supporting Information). The excellent performance obtained by the introduction of **FFF-BIm$_4$** between the emissive layer and the Al electrode is thus demonstrated.

Introduction of CPE ETLs can lead to PLEDs with temporal responses of the J and L that are on the order of seconds. For example, it is possible to observe a response time (defined as the time when J is 50% of its maximum value) of 20 s at 4 V.[5] Such a time scale is consistent with ion migration mediating device performance and, in particular, the electron injection barrier. Figure 1b compares the electroluminescence (EL) intensities vs time characteristics within a time domain of less than 20 ms observed for ITO/PEDOT/MEH-PPV/**FFF-BIm$_4$**/Al and the control device ITO/PEDOT/MEH-PPV/Ba/Al. These measurements involved applying a rectangular voltage pulse. The EL response was registered by a Si photodiode in photovoltaic regime, which was connected to an oscilloscope. Photocurrent traces were subsequently digitized by the oscilloscope. Figure 1b shows that, at least within the resolution available with our instrumentation, it was not possible to distinguish any temporal differences between the two devices. Thus, the response of the device when using **FFF-BIm$_4$** is considerably faster than that observed when using a polymeric analogue.

Atomic force microscopy (AFM) was used to examine the quality of the **FFF-BIm$_4$** layers atop MEH-PPV. Since **FFF-BIm$_4$** is an ionic molecule of intermediate dimensions, our main concern was the possibility of crystallization or poor film formation leading to rough surface features. Figure 2a shows the surface topography of the **FFF-BIm$_4$** layer atop MEH-PPV prepared under conditions identical to those for device fabrication. A rough surface is indeed obtained (rms = 12 nm); there is no indication of continuous film formation. The surface is characterized by elevated features with an average height of 39 nm, which are due to the **FFF-BIm$_4$** component. It appears that the **FFF-BIm$_4$** does not adhere well to the MEH-PPV surface, probably as a result of poor wetting or the low solution viscosity. In general these structural features are not desirable for device fabrication and would be discouraging.

Figure 2b shows the AFM image of the MEH-PPV/**FFF-BIm$_4$** surface between Al electrodes, immediately after the cathode was evaporated. These regions correspond to the areas of the organic film that were protected by the shadow mask. The surface is smooth and homogeneous, with an rms roughness of ~1.3 nm. While we recognize that the internal structure under the Al electrode is not directly probed, these measurements show that the conditions that the sample encounters during the metal evaporation process change substantially its features and lead to a fairly smooth and homogeneous surface. Consistent with this proposal is that XPS analysis of the surfaces reveals the presence of **FFF-BIm$_4$** in the regions between electrodes (Supporting Information).

In summary, we show that COEs show excellent function as the ETL in PLEDs. Indeed, ohmic-like contacts can be obtained using Al. The response time of the PLEDs is faster than that observed with CPEs. Surprisingly, we observe that the COE does not form a smooth film when cast onto MEH-PPV from a methanol solution; however this does not adversely affect the device performance. Our current thinking is that heat generated during cathode evaporation leads to thermal annealing and continuous film formation. Alternatively, complete coverage may not be a prerequisite. As suggested by the difference in performance of the ITO/PEDOT:PSS/MEH-PPV/**FFF-BIm$_4$**/Al and ITO/PEDOT:PSS/MEH-PPV/Al devices, electron injection to MEH-PPV may occur only on those regions in contact with **FFF-BIm$_4$**. Despite these uncertainties, we anticipate that the better structural and molecular control afforded by the COE may make them superior materials for ETLs, compared with their polymeric counterparts.

Acknowledgment. The authors are grateful to Mitsubishi Chemical Center for Advanced Materials (MC-CAM) and to the NSF (DMR 0606414 and DMR 0547639) for financial support.

Supporting Information Available: Synthetic and device fabrication procedures, device characteristics, XPS analysis, photographic capture of emission characteristics. This material is available free of charge via the Internet at http://pubs.acs.org.

References

(1) Pinto, M. R.; Schanze, K. S. *Synthesis* **2002**, *9*, 1293.
(2) Huang, F.; Hou, L. T.; Wu, H. B.; Wang, X. H.; Shen, H. L.; Cao, W.; Yang, W.; Cao, Y. *J. Am. Chem. Soc.* **2004**, *126*, 9845.
(3) Huang, F.; Niu, Y. H.; Zhang, Y.; Ka, J. W.; Liu, M. S.; Jen, A. K. Y. *Adv. Mater.* **2007**, *19*, 2010.
(4) Wu, H.; Huang, F.; Peng, J.; Cao, Y. *Org. Electron.* **2005**, *6*, 118.
(5) Hoven, C.; Yang, R.; Garcia, A.; Heeger, A. J.; Nguyen, T.-Q.; Bazan, G. C. *J. Am. Chem. Soc.* **2007**, *129*, 10976.
(6) (a) Pei, Q. B.; Yang, Y.; Yu, G.; Zhang, C.; Heeger, A. J. *J. Am. Chem. Soc.* **1996**, *118*, 3922. (b) Zhang, Q. S.; Zhou, Q. G.; Cheng, Y. X.; Wang, L. X.; Ma, D. G.; Jing, X. B.; Wang, F. S. *Adv. Funct. Mater.* **2006**, *16*, 1203.
(7) Zeng, W. J.; Wu, H. B.; Zhang, C.; Huang, F.; Peng, J. B.; Yang, W.; Cao, Y. *Adv. Mater.* **2007**, *19*, 810.
(8) Wang, S.; Bazan, G. C. *Adv. Mater.* **2003**, *15*, 1425.
(9) Yang, R. Q.; Wu, H. B.; Cao, Y.; Bazan, G. C. *J. Am. Chem. Soc.* **2006**, *128*, 14422.
(10) Wang, S.; Gaylord, B. S.; Bazan, G. C. *Adv. Funct. Mater.* **2003**, *13*, 463.
(11) Gong, X.; Wang, S.; Moses, D.; Bazan, G. C.; Heeger, A. J. *Adv. Mater.* **2005**, *17*, 2053.
(12) Ma, W. L.; Iyer, P. K.; Gong, X.; Liu, B.; Moses, D.; Bazan, G. C.; Heeger, A. J. *Adv. Mater.* **2005**, *17*, 274.
(13) Steuerman, D. W.; Garcia, A.; Yang, R.; Nguyen, T.-Q. *Adv. Mater.* **2008**, *20*, 528.
(14) (a) Malliaras, G. G.; Scott, J. C. *J. Appl. Phys.* **1999**, *85*, 7426. (b) Bozano, L.; Carter, S. A.; Scott, J. C.; Malliaras, G. G.; Brock, P. J. *Appl. Phys. Lett.* **1999**, *74*, 1132.

JA711068D